Measuring the scattering mean free path of Rayleigh waves on a volcano from spatial phase decoherence

Anne Obermann, Éric Larose, Ludovic Margerin, Vincent Rossetto

Geophysical Journal International

Geophys. J. Int. (2014) **197,** 435–442
Advance Access publication 2014 January 22

doi: 10.1093/gji/ggt514

Measuring the scattering mean free path of Rayleigh waves on a volcano from spatial phase decoherence

Anne Obermann,[1] Eric Larose,[1,2] Ludovic Margerin[3] and Vincent Rossetto[4,5]

[1] *University Grenoble Alpes, ISTerre, F-*38041 *Grenoble, France. E-mail: Anne.Obermann@ujf-grenoble.fr*
[2] *CNRS, ISTerre, F-*38041 *Grenoble, France*
[3] *Institut de Recherche en Astrophysique et Planétologie, Université Paul Sabatier/CNRS, Toulouse, France*
[4] *Univ. Grenoble Alpes, LPMMC,* 38042 *Grenoble, France*
[5] *CNRS, LPMMC, F-*38042 *Grenoble, France*

Accepted 2013 December 18. Received 2013 December 18; in original form 2013 August 2

SUMMARY

We analyse the statistics of phase fluctuations of seismic signals obtained from a temporary small aperture array deployed on a volcano in the French Auvergne. We demonstrate that the phase field satisfies Circular Gaussian statistics. We then determine the scattering mean free path of Rayleigh waves from the spatial phase decoherence. This phenomenon, observed for diffuse wavefields, is found to yield a good approximation of the scattering mean free path. Contrary to the amplitude, spatial phase decoherence is free from absorption effects and provides direct access to the scattering mean free path.

Key words: Surface waves and free oscillations; Coda waves; Statistical Seismology; Wave scattering and diffraction.

1 INTRODUCTION

In heterogeneous media, after a sufficient amount of time of propagation, waves enter the multiple scattering regime. In this regime waves bounce on several heterogeneities before reaching the receivers. The characteristic length (resp. time) after which such a regime can be observed is the scattering mean free path ℓ (resp. time), defined as the distance (resp. time) between two successive scattering events. This distance also refers to the characteristic distance of attenuation of the coherent wave front. The coherent wave, rigorously defined as the wave that resists ensemble averaging, roughly corresponds to the direct (or ballistic) wave. The scattering mean free path ℓ reflects the degree of heterogeneity of the medium: the longer the scattering mean free path, the weaker the scattering. ℓ depends on two features: the intensity of the fluctuations of the mechanical properties in the medium, and the spatial extension of the fluctuations. In nature, ℓ is found to vary over several orders of magnitude, depending on the frequency, and also on the nature of the material at test.

The multiple scattering regime can be observed in many fields of wave physics. It was, for instance, demonstrated in optics and in acoustics with the observation of the coherent backscattering effect (or weak localization; van Albada & Lagendijk 1985; Wolf & Maret 1985; Tourin *et al.* 1997). Seismic waves are also known to exhibit long lasting wave trains that follow ballistic *P* or *S* waves: the so-called seismic coda. Since the pioneering works of Aki (1969), the coda is known to be reproducible and has been recognized to possibly originate from multiple scattering effects. Among other applications, scattering parameters are excellent candidates for remotely characterizing geological media at depth, which is a key challenge in geosciences (Margerin & Nolet 2003). Nevertheless, in most practical cases it is very hard to discriminate scattering effects from intrinsic absorption effects. For instance, the Spatial Auto-Correlation (SPAC) technique, widely used in near-surface geophysics (Aki 1957), consists in fitting the seismic wave spatial correlation by the product of a Bessel function and an exponential decay whose physical interpretation remains debated (Prieto *et al.* 2009; Tsai 2011; Nakahara 2012). At longer distance from the source, it is also possible to study the envelope of the diffusive coda, which in principle allows one to evaluate the scattering and intrinsic attenuation (Hoshiba 1993; Carcolé & Sato 2010). In continental areas however, an unbiased estimation of these two parameters may become difficult when the leakage of scattered waves is dominant (Margerin *et al.* 1999). Although a possible remedy has been recently proposed (Del Pezzo & Bianco 2010), evaluating the scattering mean free path of a complex material without the bias of intrinsic absorption remains a challenging issue.

Recently, Anache-Ménier *et al.* (2009) studied the phase fluctuations in the coda of earthquakes recorded during a temporary experiment at the Pinyon Flats Observatory in California. They proved that seismic coda waves obey Gaussian statistics in certain frequency bands, and suggested to use the correlation of the spatial phase derivative measured in the coda to estimate the scattering mean free path. The key point of their approach is that the phase fluctuations are caused by random phase shifts acquired at each scattering event, and are therefore independent of the absorption structure. Note that the quantity of physical interest is the spatial phase difference (or derivative) and not the phase itself, because the

latter is dominated by a trivial ωt dependence, with ω the circular frequency. The determination of the scattering mean free path at Pinyon Flats was not completely conclusive because the aperture of the experimental network was less than one wavelength.

In this paper, we pursue the work of Anache-Ménier *et al.* (2009) and communicate the results of a temporary field experiment that was specially designed to measure the scattering mean free path from spatial phase decoherence. The field experiment was set up at the foot of a recent (late pleistocene and holocene) but inactive volcano in the French Auvergne in 2010. A volcanic area is particularly convenient for the study, as areas with tectonic and/or volcanic activity are highly heterogeneous and known to produce long-lasting coda waves (Aki & Chouet 1975; Goodman 1985; Abubakirov & Gusev 1990; Aki & Ferrazzini 2000). Larose *et al.* (2004) studied the weak localization of seismic waves at this site and found an estimate of 200 m for the mean free path for seismic waves around 20 Hz. This gives us a typical order of magnitude of the scattering mean free path that we can expect in our experiment.

In Section 2 we first give an overview of the theoretical aspects that underlie our study. Then, in Section 3 we describe the field experiment; prove that our signal obeys circular Gaussian statistics, the requirement to determine the scattering mean free path ℓ from spatial phase decoherence; and show the good estimate of ℓ that we obtain with our experiment (Section 3.5).

2 THEORETICAL ASPECTS

2.1 Definition of the phase

To define unambiguously the phase of the seismic wavefield $u(t, \mathbf{r})$ recorded at position $\mathbf{r}$ and time t, we introduce the associated analytic signal as follows :

$$\Psi(t, \mathbf{r}) = u(t, \mathbf{r}) + \mathrm{i}\mathrm{H}u(t, \mathbf{r}), \tag{1}$$

where i is the imaginary unit and $\mathrm{H}u(t) = \mathrm{P.V.} \int \frac{u(t')\mathrm{d}t'}{t-t'}$ denotes the Hilbert transform of the field $u(t)$. Using the polar representation of complex numbers, the field Ψ can be expressed as:

$$\Psi(t, \boldsymbol{r}) = A(t, \boldsymbol{r})\exp(\mathrm{i}\Phi(t, \boldsymbol{r})), \tag{2}$$

where $\Phi(t, \mathbf{r})$ is the wrapped phase of the field which takes values in $(-\pi : \pi]$. By correcting the phase Φ for the 2π jumps that occur at $\pm\pi$, one obtains the unwrapped phase Φ_u, which is a continuous function taking values in $\mathbb{R}$. The unwrapping operation can be performed either in the time or in the spatial domain. In this work, the field is analysed on a linear array of seismic stations, which calls for the spatial unwrapping of the phase. In general, the unwrapping operation is not topologically invariant, that is, it depends on the path from the initial to the final point. In our experiment, the path is dictated by the linear geometry of the array. Note that the phase of narrowly bandpassed signals is dominated by the term ωt—ω, the central frequency—which does not convey any interesting information on the medium. By evaluating the 'phase difference' between two nearby stations, this trivial ωt dependence is removed and the interesting fluctuations of the phase caused by the presence of heterogeneities in the medium become accessible. Motivated by this observation, we introduce two possible definitions of the phase difference. The first one, denoted by $\Delta\Phi \in (-2\pi, 2\pi]$, is obtained by subtracting the wrapped phases measured at two adjacent stations. The second one, denoted by $\Delta\Phi_u$, is obtained by unwrapping the phase spatially at each time step. Due to the finite separation between stations, it is impossible to distinguish between a large physical jump of the phase from an artefact caused by its mathematical definition. To circumvent this cycle skipping problem, we impose that the absolute value of a phase jump between two nearby stations cannot exceed π, that is, $\Delta\Phi_u$ takes values in $(-\pi, \pi]$. Using this convention, the following relations between the two definitions of the phase difference can be established:

$$\begin{aligned}
\Delta\Phi_u &= \Delta\Phi, && \Delta\Phi \in (-\pi, \pi], \\
\Delta\Phi_u &= \Delta\Phi - 2\pi, && \Delta\Phi \in (\pi, 2\pi], \\
\Delta\Phi_u &= \Delta\Phi + 2\pi, && \Delta\Phi \in (2\pi, -\pi].
\end{aligned} \tag{3}$$

2.2 Circular Gaussian statistics

Although Gaussianity is a standard hypothesis in statistical wave propagation problems, we give some heuristic arguments in support of this assumption. In the multiple scattering regime, the field u measured at a point can be considered as a superposition of a large number of partial waves ψ_α that propagated along independent paths:

$$u = \mathrm{Re}\sum_\alpha \psi_\alpha = \mathrm{Re}\sum_\alpha a_\alpha \exp(\mathrm{i}\phi_\alpha), \tag{4}$$

where the subscript α labels the different trajectories. The hypothesis that the partial waves follow independent paths is valid when the average distance between two scattering events, that is, the mean free path ℓ, is much larger than the wavelength λ. Due to the phase shift that occurs at each scattering event, after a few scattering mean free paths, the phases of the partial waves become random and uniform in the interval $(-\pi : \pi]$. In these conditions, we may apply the central limit theorem, which stipulates that the arithmetic mean of a large number of identically distributed and independent random variables will be approximately normally distributed. Hence, we conclude that the seismic coda wavefield $u(t)$ recorded at an arbitrary point of the medium can be modelled as a centred Gaussian random variable with variance $\sigma^2(t) = I(t)$, where $I(t)$ is the intensity of the coda. Because the Hilbert transform is a linear operator, it can be demonstrated that the imaginary part of the associated analytic signal obeys the same Gaussian distribution and is independent from the real part (Goodman 1985). A complex random variable, which verifies the properties just enunciated is known as Gaussian circular. Based on this observation, we now 'assume' that the complex analytic signals recorded at an arbitrary number of points at time t in the coda are jointly Gaussian circular:

$$\begin{aligned}
P(u_1, v_1, \ldots, u_N, v_N) &= P(\Psi_1, \ldots, \Psi_N) \\
&= \frac{1}{\pi^N \det(\boldsymbol{C})} \exp\left[-(\Psi_1^* \ldots \Psi_N^*)\boldsymbol{C}^{-1} \begin{pmatrix} \Psi_1 \\ \vdots \\ \Psi_N \end{pmatrix} \right],
\end{aligned} \tag{5}$$

where P denotes the probability density, $u_1 = \mathrm{Re}\Psi_1$, $v_1 = \mathrm{Im}\Psi_1$ and $\boldsymbol{C} = \langle \Psi_i \Psi_j^* \rangle$ is the covariance matrix. $(\Psi_i \ldots \Psi_N)$ are N different measurements of the field after application of a normalization procedure to be detailed below. In this work, we do not test the validity of eq. (5) in its full extent. Instead, we will derive marginal distributions for the phase and its derivative based on assumption (5), and compare the experimental measurements with the theoretical predictions to obtain estimates of the wavenumber and mean free path under the array. We also assume that different times in the coda correspond to different realizations of the underlying random

process and that temporal and statistical averaging are equivalent (ergodic hypothesis).

To complete our definition of the statistical properties of the wavefield, the covariance matrix $\boldsymbol{C}$ must be specified. Each element of the matrix depends on the two-point correlation function of the recorded wavefield u, narrowly bandpassed around circular frequency ω. In the multiple-scattering regime, the field–field correlation function in the coda may be approximated as follows:

$$\langle u(\mathbf{R}+\mathbf{x}/2,t)u(\mathbf{R}-\mathbf{x}/2,t)\rangle = \frac{S(\omega)\mathrm{e}^{-R^2/4Dt-t/t_\mathrm{a}}}{(4\pi Dt)^{d/2}}\mathrm{Im}G_d(\omega,|\mathbf{x}|), \tag{6}$$

where $S(\omega)$ is proportional to the source spectrum, $\mathbf{R}$ is the position vector connecting the source to the midpoint of the two receivers, D is the diffusion constant of the waves, t_a is their absorption time and G_d is the average Green's function of the multiple-scattering medium. The subscript d represents the space dimension and $|\cdot|$ the corresponding Euclidian distance. In our experiment u represents the vertical component of the ground displacement. Formula (6) has been demonstrated for scalar waves by Barabanenkov & Ozrin (1991) based on an eigenfunction expansion of the Bethe–Salpeter equation. Extensions to vectorial fields such as electromagnetic waves or coupled P and S waves have also been published (Barabanenkov & Orzin 1995; Margerin 2013). Physically, eq. (6) expresses the diffusive transport of the energy from the source to the array, and displays explicitly the proportionality between field–field correlations and the imaginary part of the Green's function. In seismology, the successful extraction of the surface wave part of Green's function between two stations from coda waves has been previously reported by Campillo & Paul (2003) and Paul *et al.* (2005). A very important point to be noted is that the Green's function, which appears in eq. (6), depends solely on the mean free path, at least for sufficiently weak absorption. We must now determine the correct form of G_d to be inserted in eq. (6). From our previous coherent backscattering experiment in the same area (Larose *et al.* 2004), we concluded on the dominance of Rayleigh waves in the coda. In particular, by measuring the lateral extension of the backscattering enhancement spot as a function of frequency, we were able to estimate the dispersion law of Rayleigh waves, in excellent agreement with independent estimates based on classical seismic techniques. After normalization of the two-point correlation function by the intensity received in the coda, we can write the elements of the covariance matrix as:

$$\langle \Psi_i \Psi_j^* \rangle = \bar{C}(|\mathbf{x}_j-\mathbf{x}_i|) = J_0(k|\mathbf{x}_j-\mathbf{x}_i|)\mathrm{e}^{-|\mathbf{x}_j-\mathbf{x}_i|/2l}, \tag{7}$$

where k and ℓ denote the wavenumber and mean free path of the Rayleigh waves under the array, respectively. The function $\bar{C}$ is recognized as the normalized two-point correlation function of the wavefield. The underlying 2-D character of the propagation is apparent in eq. (7). Note that the details of the intensity normalization are unimportant because the distribution of energy in the coda is spatially homogeneous at the scale of the linear array. While relation (7) gives in principle access to the mean free path ℓ, the oscillatory character of the Bessel function J_0 makes it difficult to extract the rate of decay of the exponential term in practice. The key of the method proposed by Anache-Ménier *et al.* (2009) is to remove the oscillatory term by considering the correlation of the phase derivative. The main properties of the phase and of its derivative are therefore outlined in the next paragraph.

2.3 Statistical properties of the phase

We first discuss briefly the one-point statistics ($N = 1$). We remind the reader that the real and imaginary part of the field are independent and normally distributed with zero mean and equal variance $\sigma^2 = I(t)$, which depends on the time in the coda. Although our paper focuses on the properties of the phase, it is worth recalling the marginal probability densities of other quantities derived from the complex field Ψ, as they are readily measured experimentally:

(i) The amplitude A follows a Rayleigh distribution:

$$P(A) = \frac{2A}{\langle I\rangle}\exp\left(-\frac{A^2}{\langle I\rangle}\right), \tag{8}$$

where $\langle I\rangle = \langle A^2\rangle$ is the average intensity. Using a large data set from northern Japan, Nakahara & Carcolé (2010) have demonstrated that the amplitude of coda waves is described by Rayleigh statistics with very good accuracy.

(ii) The distribution of intensity is described by a decaying exponential law:

$$P(I) = \frac{1}{\langle I\rangle}\exp\left(-\frac{I}{\langle I\rangle}\right), \tag{9}$$

which follows straightforwardly from eq. (8) after introduction of the new variable $I = A^2$.

(iii) Finally, as previously remarked, the phase Φ exhibits a uniform probability distribution:

$$P(\Phi) = \frac{1}{2\pi}. \tag{10}$$

As any oscillating signal shows a uniform phase distribution, the last property does not constitute a conclusive test of Gaussianity. In addition, we wish to point out that a wavefield obeying one-point circular Gaussian statistics does not necessarily result from multiple scattering. On the one hand, in a single scattering medium with low-contrast inclusions, the phase of the waves is not significantly modified upon scattering, and remains essentially equal to ωt, which annihilates the independent and random character of the phase. On the other hand, in a dilute scattering medium containing high-contrast inclusions, each scattering event introduces a possibly large phase shift which depends on the scattering angle, the geometry and the physical properties of the obstacle; since the phase of the singly or doubly scattered partial waves may also be considered as random, the resulting wavefield may obey Gaussian statistics and exhibit fluctuations similar to those observed in the high-order multiple scattering regime.

We now explore in more details the two-point statistics ($N = 2$). Consider two wavefields ($\Psi_1 = A_1\mathrm{e}^{\mathrm{i}\Phi_1}$, $\Psi_2 = A_2\mathrm{e}^{\mathrm{i}\Phi_2}$), recorded at geophones separated by a distance δ. Our objective is to derive the statistical properties of the phase difference $\Delta\Phi = \Phi_2 - \Phi_1$, of the unwrapped phase difference $\Delta\Phi_u$, and of the phase derivative Φ'. The correlation matrix has the following simple form:

$$\boldsymbol{C} = \begin{pmatrix} 1 & g \\ g & 1 \end{pmatrix}, \tag{11}$$

where $0 < g = \bar{C}(\delta) < 1$. The determinant and inverse of this matrix are readily calculated. Inserting these results into eq. (5), one obtains the joined distribution of the two fields:

$$P(\Psi_1,\Psi_2) = \frac{\mathrm{e}^{-|\Psi_1|^2-|\Psi_2|^2+2g\mathrm{Re}\Psi_1\Psi_2^*}}{\pi^2(1-g^2)}. \tag{12}$$

Introducing the new variables (A_1, A_2, Φ_1, Φ_2) and integrating out the phase Φ_1 yields:

$$P(A_1, A_2, \Delta\Phi) = \frac{A_1 A_2 (2\pi - |\Delta\Phi|)}{\pi^2 (1-g^2)} \mathrm{e}^{\frac{-A_1^2 - A_2^2 + 2A_1 A_2\, g \cos\Delta\Phi}{1-g^2}}, \quad (13)$$

where $\Delta\Phi \in (-2\pi, 2\pi]$. To eliminate the remaining variables A_1 and A_2, it is convenient to introduce polar coordinates $A_1 = r\cos\theta$, $A_2 = r\sin\theta$ with $\theta \in [0, \pi/2]$. The integration over (r, θ) is a straightforward computational exercise and the final result is:

$$P(\Delta\Phi) = \frac{N(1-g^2)}{1-f^2}\left(1 + \frac{f \arccos -f}{\sqrt{1-f^2}}\right), \quad (14)$$

where $N = (2\pi - |\Delta\Phi|)/4\pi^2$. Note that the distribution of the unwrapped phase difference $\Delta\Phi_u$ is easily obtained using relations (3), and is formally identical to that of $\Delta\Phi$ with $N = 1/2\pi$. In the limit $\delta \to 0$, we may expand the phase difference $\Delta\Phi \approx \Phi'\delta$ and the correlation coefficient $g \approx 1 - Q\delta^2/2$, where Φ' represents the first spatial derivative of the phase and $Q = -\bar{C}''(0)$. Note that since the correlation function $\bar{C}$ is even, the correlation coefficient g must be expanded to second-order in the small parameter δ. Upon reporting these approximations into eq. (13), and applying a Taylor series expansion around $\delta = 0$, we obtain the statistics of the first phase derivative:

$$P(\Phi') = \frac{Q}{2(Q + \Phi'^2)^{3/2}}. \quad (15)$$

Remarkably, the first spatial derivative of the phase depends on only one parameter Q. Using the expression (7) for $\bar{C}$, we obtain $Q = k^2/2(1 - 2/(kl)^2) \approx k^2/2$. The last approximation is valid because the mean free path is in general much larger than the wavelength. This means that within the experimental accuracy, the measurement of Q does not put constraints on the mean free path. For sufficiently large values of the phase derivative, the probability density (15) is independent of the parameter Q and follows a power-law decay $P(\Phi') \sim \Phi'^{-3/2}$, characteristic of circular Gaussian statistics.

We now outline the derivation of the correlation function of the spatial phase derivative along the array. The method is analogous to the one employed to derive eq. (14) but the calculations are far more complex. We provide the key ingredients and refer the interested reader to the work of van Tiggelen *et al.* (1999) for more details. The first step is the calculation of the correlation matrix of four fields Ψ_i ($i = 1, 2, 3, 4$) acquired at four positions: $x_1, x_1 + \delta, x_3, x_3 + \delta$. Using expression (7), we obtain:

$$\boldsymbol{C}(x,\delta) = \begin{pmatrix} 1 & \bar{C}(\delta) & \bar{C}(x) & \bar{C}(x+\delta) \\ -\bar{C}(\delta) & 1 & \bar{C}(x-\delta) & \bar{C}(x) \\ -\bar{C}(x) & -\bar{C}(x-\delta) & 1 & \bar{C}(\delta) \\ -\bar{C}(x+\delta) & -\bar{C}(x) & -\bar{C}(\delta) & 1 \end{pmatrix}, \quad (16)$$

where $x = x_3 - x_1$. Using a perturbation approach, the eigenvectors and associated eigenvalues of the matrix (16) are calculated to first and second order in the small parameter δ, respectively. In this way, the joint probability distribution of the fields and of their spatial derivatives $(\Psi(x_1),\Psi(x_3),\Psi'(x_1),\Psi'(x_3))$ can be calculated. Introducing the polar representation $\Psi(x_i) = A(x_i)\mathrm{e}^{\mathrm{i}\Phi(x_i)}$, the joint probability distribution $P(A_1, A_1', A_3, A_3', \Phi_1, \Phi_1', \Phi_3, \Phi_3')$ of the amplitude and phase at x_1 and x_3 together with their spatial derivatives is obtained. Note that this probability density depends on $x = x_3 - x_1$ only. After integration over the amplitudes, amplitude derivatives and phases, the correlation function of the phase derivative may be expressed as (van Tiggelen *et al.* 2006):

$$C_{\Phi'}(x) = \iint_{-\infty}^{+\infty} P(\Phi_1', \Phi_3')\Phi_1'\Phi_3' \mathrm{d}\Phi_1'\mathrm{d}\Phi_3'$$
$$= \frac{1}{2}\log(\bar{C}(x))''(\log(1 - \bar{C}(x)^2)). \quad (17)$$

For sufficiently large x, the exact expression (17) can be approximated as follows:

$$C_{\Phi'}(x) \approx \frac{\mathrm{e}^{-|x|/l}}{2|x|}. \quad (18)$$

As anticipated, the oscillatory term $J_0(k|x|)$ does not show up in eq. (18). Using numerical simulations, Anache-Ménier *et al.* (2009) have demonstrated that the convenient formula (18) applies for $x > \lambda/5$. Hence, correlations of the spatial derivative of the phase provide direct access to the mean free path. Two very important remarks must be made at this point. To derive eq. (18), we have implicitly assumed that translational invariance applies. If the statistical properties vary under the array, the result (18) may well be invalid. The second point pertains to the evaluation of the spatial derivative of the field. Throughout the derivation of eq. (18), we have assumed that the derivatives are evaluated in the direction of the array. The correlation function of the 'directional' derivative of the phase at an angle α with respect to the array direction gives a quite different result. In particular the undesirable oscillations of the correlation $\bar{C}$ are not suppressed in this case (Ghysels 2005).

3 EXPERIMENT AND RESULTS

3.1 Experiment setup and data acquisition

We work at the foot of the neighbouring volcanic craters 'Grand Sarcoui' and "Puy des Goules" in the French Auvergne. Larose *et al.* (2004) could show the evidence ofthe weak localization of seismic waves in this area (at 20 Hz) and gave hence a proof of multiple scattering. To measure the scattering mean free path from phase decoherence, we set up an experiment that simultaneously fulfills two conditions: (1) The intergeophone spacing must be sufficiently small to ensure a good correlation of the signals at neighbouring geophones; (2) The total aperture of the array should not be too small compared to the mean free path. From numerical simulations with a finite difference code (Derode *et al.* 2003), we observed that the intergeophone spacing δ should be $\delta \leq \lambda/10$, where λ is the Rayleigh wavelength, and that an increasing number of geophones significantly increases the precision of the determination of ℓ.

We see that it is essential to know the Rayleigh wavelength in the area of interest. Therefore, in a preliminary study, we shot 20 refraction seismic profiles (hammer source) in the area of interest. We then computed the dispersion curves: once by determining the wavenumbers from the field correlation (eq. 7) at different central frequencies, and once from a frequency–wavenumber analysis. From these analysis, we could determine an approximated wavelength of 24 m at 10 Hz, 11 m at 20 Hz and 7.5 m at 30 Hz.

We hence decided to work at high frequencies (30 Hz) and set up a linear array of 48 geophones along an unpaved road at the foot of the volcanoes with an intergeophone spacing of $\delta = 60$ cm ($\approx\lambda/10$). The total length of the array is 28.8 m, which is approximately four times the dominant wavelength at 30 Hz. To decrease the ambient noise, we buried the geophones at 20 cm depth. We

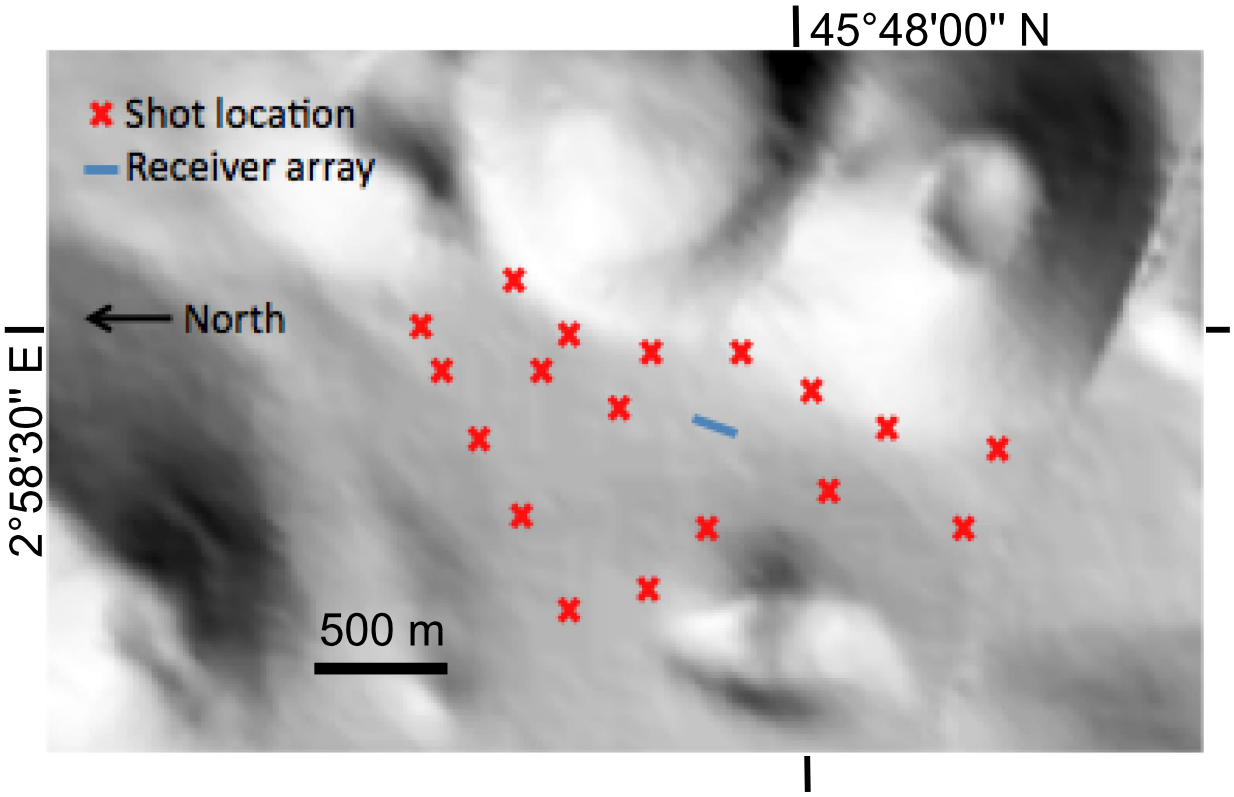

Figure 1. Area of interest in Auvergne. The blue line marks the array of 48 geophones with 0.6 m spacing. The red stars mark the positions of the 18 explosive sources placed around the geophones.

placed 18 explosives on unpaved roads around the receiver array to excite energy from all directions. The experimental setup is shown in Fig. 1. The acquired data show long-lasting coda waves with a high signal-to-noise ratio for the first 20 s in the coda (Fig. 2).

For our analysis we assume a 2-D medium. This approach is valid as long as the vertical component of our signals is largely dominated by Rayleigh waves (Larose *et al.* 2004).

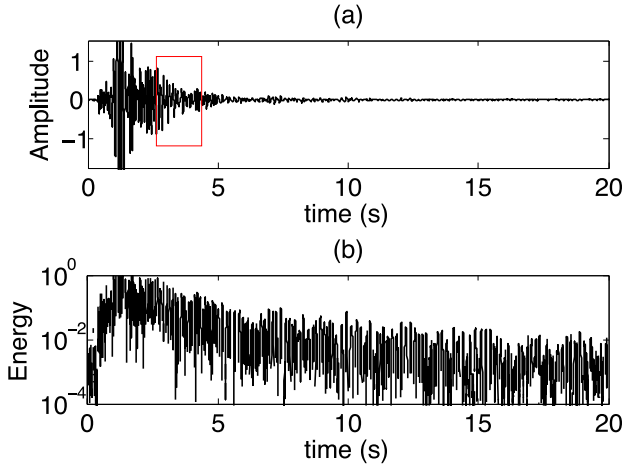

Figure 2. (a) Raw data from an explosive source, showing a coda of 20 s. The square indicates the chosen time window in the coda. (b) Dimensionless energy of the signal.

3.2 Test of one-point Circular Gaussian Statistics

To begin with, we test that the seismic coda waves that we acquired obey Circular Gaussian Statistics. Therefore, we filter the data with a narrow second-order bandpass filter of 5 per cent around a central frequency of 30 Hz.

We selected a short time window of 1.5 s starting after the surface wave arrivals. We compute the imaginary part (Hilbert transform) of the recorded signals $u(t, \mathbf{r})$ that gives us access to the phase from the complex analytical signals (eq. 4). We can define:

(i) The wrapped phase Φ, which is the argument of the complex field u in the range $(-\pi, \pi]$.

(ii) The unwrapped phase Φ_u, that is obtained by correcting for the 2π jumps that occur when Φ goes through $\pm\pi$. The result is a continuous function.

We then test the criteria for Circular Gaussian Statistics, as mentioned in Section 2.2. The results for the different tests are shown in Fig. 3 together with the theoretical predictions. We can see that:

(i) The real and imaginary part of the field follow a Gaussian distribution (Figs 3a and b) and are independent (Fig. 3c).

(ii) The amplitude presents a Rayleigh distribution (Fig. 3d). There are only small discrepancies for larger amplitudes that result from superimposed noise.

(iii) The intensity is calculated as the squared amplitude of the Hilbert transformed signal. Its distribution clearly follows a decaying exponential probability function (Fig. 3e).

(iv) The probability distribution of the phase is uniform with a value of $1/2\pi$ (Fig. 3f).

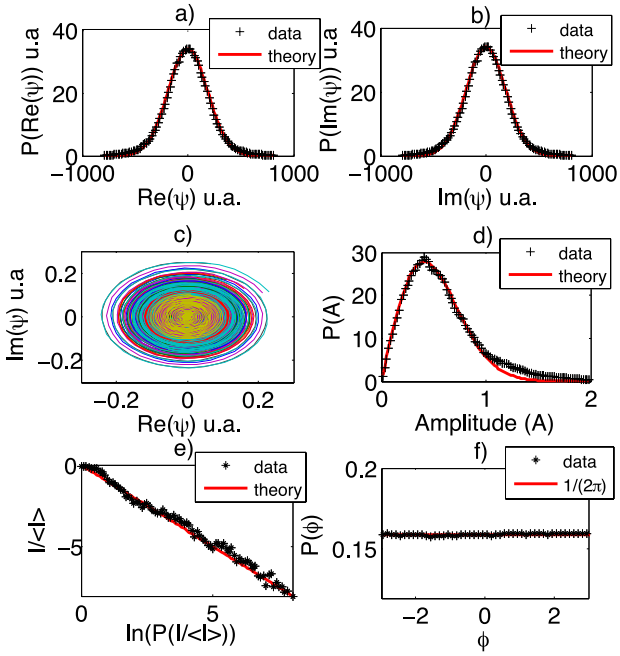

Figure 3. Criteria for a signal that obeys circular Gaussian statistics: (a) Gaussianity of the real part; (b) Gaussianity of the imaginary part; (c) circular dependence of real and imaginary part; (d) Rayleigh distribution of the amplitude; (e) intensity distribution follows a decaying exponential probability function and (f) uniform phase distribution.

We mentioned in Section 2.2 that the phase distribution is an ambiguous test for the Gaussian character of a signal, as every oscillating signal shows a uniform phase distribution. We will hence also test the phase derivative distribution to verify that the seismic coda obeys Circular Gaussian Statistics.

3.3 Field correlation

We compute the field correlation (eq. 7) for all possible receiver combinations. As the length of our whole array is only four wavelengths, this might not be enough to average over the heterogeneities, and result in a lack of translation symmetry. In Fig. 4 we display the field correlation averaged over three shots that showed similar behaviour. From the zero passage of the wave we can determine a wavelength of 8 m, which is in good agreement with the results from the preliminary analysis. From Fig. 4 we can also determine the correlation coefficient $C(\delta) = \langle \Psi(r-\delta/2)\Psi^*(r+\delta/2)\rangle$

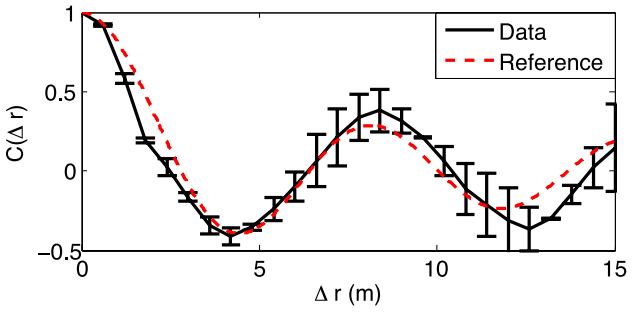

Figure 4. Field correlation. The zero passage reveals a wavelength of about 8 m. From the correlation coefficient between adjacent receivers (0.6 m), we can obtain the parameter $g = 0.93$.

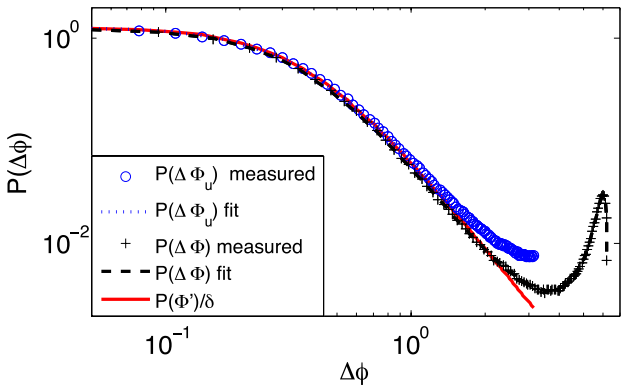

Figure 5. Unwrapped $P(\Delta\Phi_u)$ and wrapped $P(\Delta\Phi)$ phase difference distribution plotted together with the theoretical distribution and the analytical phase derivative $P(\Phi')$.

between adjacent receivers ($\delta = 0.6$ m) as $C(\delta = 0.6\,\text{m}) = 0.93 = g$ (at 30 Hz). We will use this parameter g now as fitting parameter for the finite difference calculation of the phase derivative.

3.4 First phase derivative distribution

As we cannot determine the phase derivative analytically from our data, we use a finite-difference approach in space ($P(\Phi') \approx P(\Delta\Phi)/\delta$). We can use both, the wrapped and the unwrapped phase, to estimate the spatial derivative of the phase from the simple finite-difference formula $\Phi' \approx \Delta\Phi/\delta$ and $\Phi'_u \approx \Delta\Phi_u/\delta$, respectively. $\Delta\Phi$ and $\Delta\Phi_u$ are the differences of the phases between two seismometers that are separated by a distance δ. We recall that the theoretical formulation for the phase difference distribution is given in eq. (14).

In Fig. 5 we show the wrapped and unwrapped phase finite-difference distributions, together with the theoretical phase difference distribution $P(\Delta\Phi)$ (eq. 14), and the analytical derivative distribution $P(\Phi')$ (eq. 15). The distributions $P(\Delta\Phi)$ and $P(\Delta\Phi_u)$ are symmetric and therefore just represented for positive values in a logarithmic scale. We note that the analytical derivative is followed longer by the wrapped phase. We use the fitting parameters $g = 0.93$ (obtained from the field correlation), and $Q \approx \frac{2\pi^2}{\lambda^2} = 0.3\ \text{m}^{-2}$ with $\lambda = 8$ m (from field correlation, preliminary seismic refraction experiment). The agreement of the theoretical distributions and the data is excellent and we can conclude that our field satisfies two-point Circular Gaussian Statistics with good accuracy.

3.5 Phase derivative correlations

To compute the phase difference correlation, we work with the spatially unwrapped phase Φ_u, as the wrapped phase is dominated by 2π jumps of geometrical and not physical origin. We compute the correlations between all possible receiver combinations, separately for each shot, and then average correlations from the same receiver distances. Anache-Ménier *et al.* (2009) have shown with numerical simulations, that the asymptotic exponential regime is already reached for $r > \lambda/5$. As the aperture of our experimental network is several wavelength in size, we can in principle measure the scattering mean free path directly from the slope $(-1/\ell)$ of the phase derivative decay as a function of distance in logarithmic scale. However, since the fluctuations of our measurements are very large, we do not attempt to determine exactly the value of ℓ, but instead try to provide an estimate of its order of magnitude.

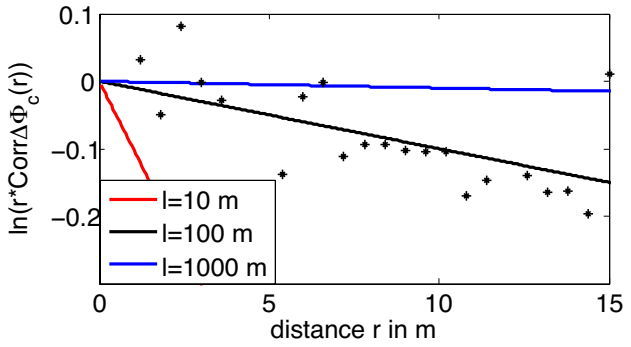

Figure 6. Phase difference correlation for 48 receivers with 0.6 m spacing in logarithmic representation multiplied by the distance. Superimposed are the theoretical distributions for three different scattering mean free paths ($\ell = 10$, 100, 1000 m).

In Fig. 6 we plot the phase difference correlation in logarithmic scale versus the distance. We multiplied the correlation with r, so that the slope is directly proportional to $-1/\ell$. We superpose theoretical predictions (eq. 18) for three scattering mean free paths (10, 100 and 1000 m) on the data in Fig. 6. In spite of the large fluctuations, we can reasonably exclude 10 m and 1000 m as possible values for ℓ. $\ell \approx$100 m seems to be a good approximation and is in agreement with previous findings by Larose *et al.* (2004). A more precise determination is unfortunately not possible with the limited number of receivers and shots in our experiment.

4 CONCLUSION

In this paper, we demonstrate that the correlation function of the spatial derivative offers a new, promising opportunity to measure directly the scattering mean free path ℓ of a given heterogeneous medium. This measurement is independent of the absorption length and offers access to the scattering properties of the medium. In future applications, the ideal configuration should consist of a much larger number of receivers, to cover at least 10 λ. The interstation distance of the order of $\lambda/10$ proved to be good enough to keep a high correlation between two nearby stations and to reduce systematic errors in the derivatives. Our method may find applications in various areas of seismology where the effects of scattering are prominent and a knowledge of the scattering properties is necessary to describe the propagation. As an example, an unbiased estimate of the scattering mean free path is crucial for the localization of changes in multiply scattering media, where a sensitivity kernel based on diffusion theory is used (Larose *et al.* 2010; Obermann *et al.* 2013a,b). Our experimental approach may also provide independent estimates of the scattering mean free path in volcanic areas where particularly strong scattering has been proposed, based on the fitting of energy envelopes using energy transport approaches (Wegler & Lühr 2001; Yamamoto & Sato 2010).

ACKNOWLEDGEMENTS

This work was funded by the ANR JCJC SISDIF grant. The experiment was deployed under the supervision of A. Mariscal and I. Douste-Bacquet. We wish to thank D. Anache-Ménier and B. van Tiggelen for enlightening discussions and support.

REFERENCES

Abubakirov, I.R. & Gusev, A.A., 1990. Estimation of scattering properties of lithosphere of Kamchatka based on Monte-Carlo simulation of record envelope of a near earthquake, *Phys. Earth planet. Inter.,* **64**(1), 52–67.

van Albada, M.P. & Lagendijk, A., 1985. Observation of weak localization of light in a random medium, *Phys. Rev. Lett.,* **55,** 2692–2695.

Aki, K., 1957. Space and time spectra of stationary stochastic waves, with special reference to microtremors, *Bull. Earthq. Res. Inst.,* **35,** 415–456.

Aki, K., 1969. Analysis of seismic coda of local earthquake as scattered waves, *J. geophys. Res,* **74**(2), 615–631.

Aki, K. & Chouet, B., 1975. Origin of coda waves: source, attenuation and scattering effects, *J. geophys. Res,* **80**(23), 3322–3342.

Aki, K. & Ferrazzini, V., 2000. Seismic monitoring and modeling of an active volcano for prediction, *J. geophys. Res.,* **105**(B7), 16 617–16 640.

Anache-Ménier, D., van Tiggelen, B.A. & Margerin, L., 2009. Phase statistics of seismic coda waves, *Phys. Rev. Lett.,* **102**(248501), 1–4.

Barabanenkov, Y.N. & Ozrin, V., 1991. Asymptotic solution of the Bethe-Salpeter equation and the Green-Kubo formula for the diffusion constant for wave propagation in random media, *Phys. Lett. A,* **154**(1), 38–42.

Barabanenkov, Yu.N. & Orzin, V.D., 1995. Diffusion asymptotics of the Bethe-Salpeter equation for electromagnetic waves in discrete random media, *Phys. Lett. A.,* **206,** 116–122.

Campillo, M. & Paul, A., 2003. Long-range correlations in the diffuse seismic coda, *Science,* **299,** 547–549.

Carcolé, E. & Sato, H., 2010. Spatial distribution of scattering loss and intrinsic absorption of short-period S-waves in the lithosphere of Japan on the basis of the Multiple Lapse Time Window Analysis of Hi-net data, *J. geophys. Res.,* **180**(1), 268–290.

Del Pezzo, E. & Bianco, F., 2010. Two-layer earth model corrections to the MLTWA estimates of intrinsic-and scattering-attenuation obtained in a uniform half-space, *Geophys. J. Int.,* **182**(2), 949–955.

Derode, A., Larose, E., Tanter, M., de Rosny, J., Tourin, A., Campillo, M. & Fink, M., 2003. Recovering the Green's function from field-field correlations in an open scattering medium, *J. acoust. Soc. Am.,* **113**(6), 2973–2976.

Ghysels, A., 2005. Propagation des ondes sismiques: analyse de la phase aléatoire, *PhD thesis,* Universitdé Grenoble.

Goodman, J.W., 1985. *Statistical Optics, Wiley Series in Pure and Applied Optics,* Wiley.

Hoshiba, M., 1993. Separation of scattering attenuation and intrinsic absorption in japan using the multiple lapse time window analysis of full seismogram envelope, *J. geophys. Res.,* **98,** 809–824.

Larose, E., Derode, A., Campillo, M. & Fink, M., 2004. Imaging from one-bit correlations of wide-band diffuse wavefields, *J. appl. Phys.,* **95**(12), 8393–8399.

Larose, E., Planès, T., Rossetto, V. & Margerin, L., 2010. Locating a small change in a multiple scattering environment, *Appl. Phys. Lett.,* **96**(204101), 1–3.

Margerin, L., 2013. Diffusion approximation with polarization and resonance effects for the modelling of seismic waves in strongly scattering small-scale media, *Geophys. J. Int.,* **192**(1), 326–345.

Margerin, L. & Nolet, G., 2003. Multiple scattering of high-frequency seismic waves in the deep Earth: modeling and numerical examples, *J. geophys. Res,* **108**(B5), 2234, doi:10.1029/2002JB001974.

Margerin, L., Campillo, M., Shapiro, N.M. & van Tiggelen, B., 1999. Residence time of diffuse waves in the crust and the physical interpretation of coda Q. Application to seismograms recorded in Mexico, *Geophys. J. Int.,* **138,** 343–352.

Nakahara, H., 2012. Formulation of the spatial autocorrelation (SPAC) method in dissipative media, *Geophys. J. Int.,* **190**(3), 1777–1783.

Nakahara, H. & Carcolé, E., 2010. Maximum-likelihood method for estimating coda q and the Nakagami-m parameter, *Bull. seism. Soc. Am.,* **100**(6), 3174–3182.

Obermann, A., Planès, T., Larose, E. & Campillo, M., 2013a. Imaging pre- and co-eruptive structural and mechanical changes on a volcano with ambient seismic noise, *J. geophys. Res.,* **118,** 1–10.

Obermann, A., Planès, T., Larose, E., Sens-Schönfelder, C. & Campillo, M., 2013b. Depth sensitivity of seismic coda waves to velocity perturbations in an elastic heterogeneous medium, *Geophys. J. Int.,* **194**(1), 372–382.

Paul, A., Campillo, M., Margerin, L., Larose, E. & Derode, A., 2005. Empirical synthesis of time-asymmetrical green functions from the correlation of coda waves, *J. geophys. Res.,* **110**(B8), B08302, doi:10.1029/2004JB003521.

Prieto, G.A., Lawrence, J.F. & Beroza, G.C., 2009. Anelastic Earth structure from the coherency of the ambient seismic field, *J. geophys. Res.,* **114**(B7), doi:10.1029/2008JB006067.

van Tiggelen, B., Sebbah, P., Stoytchev, M. & Genack, A., 1999. Delay-time statistics for diffuse waves, *Phys. Rev. E,* **59,** 7166–7172.

van Tiggelen, B.A., Anache-Ménier, D. & Ghyssels, A., 2006. Role of mean free path in spatial phase correlation and nodal screening, *Europhys. Lett.,* **74,** 999–1005.

Tourin, A., Derode, A., Roux, P., van Tiggelen, B.A. & Fink, M., 1997. Time-dependent coherent backscattering of acoustic waves, *Phys. Rev. Lett.,* **79,** 3637–3639.

Tsai, V.C., 2011. Understanding the amplitudes of noise correlation measurements, *J. geophys. Res.,* **116**(B09311), doi:10.1029/2011JB008483.

Wegler, U. & Lühr, B.G., 2001. Scattering behaviour at Merapi volcano (Java) revealed from an active seismic experiment, *Geophys. J. Int.,* **145**(3), 579–592.

Wolf, P. & Maret, G., 1985. Weak localization and coherent backscattering of photons in disordered media, *Phys. Rev. Lett.,* **55,** 2696–2699.

Yamamoto, M. & Sato, H., 2010. Multiple scattering and mode conversion revealed by an active seismic experiment at Asama volcano, Japan, *J. geophys. Res.,* **115**(B7), doi:10.1029/2009JB007109.